HHS Public Access

Author manuscript

Proteins. Author manuscript; available in PMC 2016 May 19.

Published in final edited form as:

Proteins. 2013 August ; 81(8): 1304–1317. doi:10.1002/prot.24264.

Computationally-predicted CB1 cannabinoid receptor mutants show distinct patterns of salt-bridges that correlate with their level of constitutive activity reflected in G protein coupling levels, thermal stability, and ligand binding

Kwang H. Ahn[1], **Caitlin E. Scott**[2], **Ravinder Abrol**[2], **William A. Goddard III**[2], and **Debra A. Kendall**[1,*]

[1] Department of Pharmaceutical Sciences, University of Connecticut, Storrs, Connecticut

[2] Materials and Process Simulation Center, California Institute of Technology, Pasadena, California

Abstract

The cannabinoid receptor 1 (CB1), a member of the class A G-protein-coupled receptor (GPCR) family, possesses an observable level of constitutive activity. Its activation mechanism, however, has yet to be elucidated. Previously we discovered dramatic changes in CB1 activity due to single mutations; T3.46A, which made the receptor inactive, and T3.46I and L3.43A, which made it essentially fully constitutively active. Our subsequent prediction of the structures of these mutant receptors indicated that these changes in activity are explained in terms of the pattern of salt-bridges in the receptor region involving transmembrane domains 2, 3, 5, and 6. Here we identified key salt-bridges, R2.37 + D6.30 and D2.63 + K3.28, critical for CB1 inactive and active states, respectively, and generated new mutant receptors that we predicted would change CB1 activity by either precluding or promoting these interactions. We find that breaking the R2.37 + D6.30 salt-bridge resulted in substantial increase in G-protein coupling activity and reduced thermal stability relative to the wild-type reflecting the changes in constitutive activity from inactive to active. In contrast, breaking the D2.63 + K3.28 salt-bridge produced the opposite profile suggesting this interaction is critical for the receptor activation. Thus, we demonstrate an excellent correlation with the predicted pattern of key salt-bridges and experimental levels of activity and conformational flexibility. These results are also consistent with the extended ternary complex model with respect to shifts in agonist and inverse agonist affinity and provide a powerful framework for understanding the molecular basis for the multiple stages of CB1 activation and that of other GPCRs in general.

Keywords

GPCR; constitutive activity; protein structure prediction; ligand binding; G-protein coupling; thermal stability

[*]Correspondence to: Debra A. Kendall, Department of Pharmaceutical Sciences, 69 N. Eagleville Road, Storrs, CT 06269-3092. ; Email: debra.kendall@uconn.edu..

INTRODUCTION

G protein-coupled receptors (GPCRs) play a central role in biological processes by transmitting signals from various external stimuli, including neurotransmitters, hormones, and light, across the cell membrane. The cannabinoid receptor one (CB1) is a member of the rhodopsin-like GPCR family that binds Δ^9-THC, the psychoactive component of marijuana, and exerts its pharmacological effects via intracellular signaling cascades. CB1 is one of the most abundant GPCRs in the mammalian brain and is found in the basal ganglia, cerebellum, and hippocampus. Like other GPCRs, activation by agonists, induces CB1 to undergo conformational changes that promote activation of the coupled guanine nucleotide-binding protein (G-protein) which then stimulates downstream effector proteins, such as inhibition of adenylate cyclase activity and calcium channels and activation of inwardly rectifying potassium channels.[1]

Early thinking about GPCR function assumed the existence of just two GPCR states, the “off” (R) and “on” (R*) modes representing the inactive and active states of the receptor, respectively.[2] This binary complex model suggests that an agonist shifts the equilibrium in favor of the active form of the receptor that can couple to G-protein. This model was later extended to account for the activity of constitutively active mutant (CAM) receptors that can couple to G-protein in a ligand-independent manner.[3,4] Since CAMs are pre-coupled to G protein, they are characterized by enhanced affinity for agonists, decreased affinity for inverse agonists, and increased basal functional activity. Interestingly, CAMs are known for many GPCRs, including rhodopsin,[5] β_1 adrenergic receptor,[6] histamine H1 receptor,[7] angiotensin receptor type 1,[8] opioid receptor,[9] and the CB1 cannabinoid receptor.[10,11] More recently it has become clear that GPCRs can adopt multiple distinct conformations displaying different states of receptor activation resulting in different signaling efficacies.[12] Thus, the transition from inactive to active forms of a GPCR may include several distinct conformational substates that can be differentially stabilized by G proteins or by different ligands – opening the way for highly selective therapeutic agents—or by mutations that stabilize a particular receptor conformation.[13–15] Many GPCRs[16,17] including the CB1 receptor[18] possess constitutive activity in the absence of ligand. Therefore, wild-type CB1 is at a pivot point and can become more fully activated by agonists such as CP55940 and Δ^9-THC or inhibited by the inverse agonists SR141716A and AM251.[19] Using the wild-type and mutant forms of the CB1 receptor, this study presents for the first time a detailed activation mechanism that provides a structural basis for the constitutive activity exhibited by GPCRs, how they become fully inactive, and what structural changes allow them to become more active.

We previously showed that the single amino acid substitution of leucine at position 3.43 with alanine, or of threonine 3.46 with isoleucine, caused the slightly active CB1 receptor to become highly constitutively active.[10,11] Note the positions of the transmembrane (TM) helix residues are indicated using the Ballesteros-Weinstein amino acid numbering system[20] throughout the text. In this numbering system, the most conserved residue in each TM helix is given the location of 0.50. This number is preceded by the TM number. All other residues in the TM helix are numbered relative to this residue. Thus, the L3.43 and T3.46 residues are approximately two and one turn above, respectively, the arginine residue of the highly

conserved DRY motif in TM3, which has been shown to form ionic interactions with the glutamic acid residues at position 3.49 and 6.30 in the crystal structure of inactive rhodopsin.[21] In contrast, we showed that an alanine substitution of T3.46 resulted in a fully inactive receptor. Consistent with the characteristics of a CAM, the more active T3.46I and L3.43A receptors show enhanced and decreased affinities for agonists and inverse agonists, respectively, relative to the wild-type receptor while the inactive T3.46A receptor exhibits the reverse profile.

To interpret the dramatic changes in function observed for the wild-type, L3.43A, T3.46A, and T3.46I receptors, we used the GEnSeMBLE (GPCR Ensemble of Structures in Membrane Bilayer Environment) method[22] to predict the three-dimensional structures of their TM domains and found that their stability and activity correlates with the predicted pattern of key salt-bridges.[23] Our previous study shows that the differences between the active and inactive predicted structures agree well with those observed between active and inactive crystallographically characterized GPCRs,[21,24–38] giving credence to the predicted structures. While many diverse types of contacts and interhelical interactions stabilize each activation state, our work focuses on the salt-bridges, especially the intracellular ones. Changes in hydrophobic interactions, aromatic stacking, and hydrogen bonds in the TM bundle are important, but they do not provide the strongest indication for activation.

Our computational predictions of CB1 suggest that transition between distinct patterns of salt-bridges is critical for receptor activity. Based on these predicted structures and the hypothesis that the salt-bridges control the propensity for activation, we predicted a series of new CB1 mutants expected to either preclude or promote these ionic interactions which we expected to exhibit specific levels of constitutive activity relative to the wild-type receptor. Indeed, our computational structural prediction data showed the pattern of key salt-bridges is conserved among the mutant receptors that are expected to have a similar level of constitutive activity suggesting those may be critical for receptor activation. In particular, the R2.37 + D6.30 and D2.63 + K3.28 salt-bridges are identified in inactive and active CB1 receptors, respectively. We then experimentally constructed these mutants to break these salt-bridges and found that they exhibit substantial shifts in G protein coupling, thermal stability, and ligand binding affinity relative to the wild-type, consistent with our expected changes in constitutive activity and conformational flexibility. This excellent correlation of experimental activation propensity with the role of key salt-bridges in our predicted structures provides new insight into the interconnection between structure and function of CB1. These results support and extend the concepts of the extended ternary complex model with respect to shifts in agonist and inverse agonist affinity.[6,39,40] This provides a new powerful framework for understanding the molecular basis for the stages of CB1 activation in particular and by inference that of other GPCRs.

MATERIALS AND METHODS

Receptor structure prediction

The structures of CB1 wild-type and mutant receptors were predicted as described previously.[23] The ensemble of low energy conformations of each receptor was predicted using the first-principles based GEnSeMBLE method.[22] All simulations used the Dreiding

force field.[41] The ensemble of the best 10 conformations (by lowest energy) for each mutant was analyzed in detail for the presence of salt-bridge, hydrogen-bond, and hydrophobic interactions. Briefly, the seven individual TMs were predicted based on the octanol hydrophobicity scale[42] using the PredicTM[22] method and extended using helical structure predictions from three secondary structure prediction servers: Porter Protein Secondary Structure Prediction Server,[43,44] APSSP2: Advanced Protein Secondary Structure Prediction Server,[45,46] and PSIPRED: Protein Prediction Server.[47–49] The separate helices were built and optimized with OptHelix[22] before the TMs aligned to multiple crystal templates. We compared the energies resulting from the turkey beta 1 adrenergic receptor, bovine rhodopsin receptor, human β_2 adrenergic receptor, and human adenosine A_{2A} receptor templates because they were the only crystallographically characterized GPCRs available at the time of these computational studies. The turkey β_1 adrenergic receptor crystal provided the lowest energy helix packing conformations for the wild-type CB1 receptor, which is a reasonable result because out of the four receptors, the turkey β_1 adrenergic receptor had the highest percentage identity of conserved TM residues with respect to the CB1 wild-type receptor at 28.45%. We completed the following procedure with this template.

To predict the structures of single and double mutant receptors, the target residues were mutated in the OptHelix optimized TM2 or TM3 from the wild-type receptor using SCREAM (Side Chain Rotamer Excitation Analysis Method).[50] Each helix rotation angle (η) was sampled using the BiHelix method,[51] where the side chain rotamers were optimized using SCREAM. For the lowest energy conformation from the BiHelix protocol, we performed a local sampling of helix tilt angle (θ), sweep angle (ϕ), and rotation angle (η) for all pairs of interacting helices while optimizing the side chain rotamers using SCREAM. From this, the top 2000 conformations were selected and reordered using more accurate conformational energies obtained by explicitly constructing the 7-helix bundles. Each of them was minimized for 10 steps in a vacuum. Finally, the 10 lowest energy structures were selected according to the average energy rank. Four different types of energies were calculated for each minimized receptor including the charged total energy, the neutralized total energy, the charged interhelical energy, and the neutralized interhelical energy. The total energy refers to the energy of the entire receptor, whereas the interhelical energy is defined as the energy between interacting helices. In the charged state, the acidic residues (glutamic acid and aspartic acid) have a negative charge, and the basic residues (lysine, protonated histidine, and arginine) have a positive one. Under the neutralized conditions, the acidic residues gain a hydrogen atom and the basic residues lose one. Each receptor is ranked according to these four energy types, and these respective ranks are averaged to give a final rank representing the average energy rank. We examined a small selection of 10 final receptor conformations. These 10 receptors are found to all share similar characteristics, which define the “consensus structure.” The receptor conformations shown in Figure 1(A) are those that faithfully represent the consensus structure.

CB1 expression and membrane preparation

The plasmid DNA encoding human CB1 receptors was prepared as previously described.[52] HEK293 cells were grown in Dulbecco's modified Eagle's medium supplemented with 10% fetal bovine serum and 3.5 mg/mL glucose at 37°C in 5% CO_2. For transient expression of

the receptors, HEK293 cells were seeded at 1 million cells/100 mm dish on the day prior to transfection using the calcium phosphate precipitation method.[53] Twenty-four hours post-transfection, membranes of transfected cells expressing the wild-type or mutant receptors were prepared using nitrogen cavitation as previously described.[10]

GTPγS binding assay

Approximately 5 μg of membrane preparations from HEK293 cells expressing CB1 receptors were incubated for 60 min at 30°C in a total volume of 500 μL GTPγS binding assay buffer (50 m*M* Tris-HCl, pH 7.4, 3 m*M* $MgCl_2$, 0.2 m*M* EGTA, and 100 m*M* NaCl) with 0.1 n*M* [^{35}S]GTPγS (1250 Ci/mmol, PerkinElmer Life Sciences, Boston, MA), 1 μ*M* GDP, and 0.1% (w/v) BSA. The levels of basal and CP55940-induced GTPγS binding were measured in the absence of ligand and presence of 1 μM unlabeled CP55940, respectively. Non-specific binding was determined with 10 μ*M* unlabeled GTPγS (Sigma, St Louis, MO). The reaction was terminated by rapid filtration to separate the membrane-bound fraction from the free through Whatman GF/C filters (Brandel Inc., Gaithersburg, MD). The radioactivity of the membrane-bound [^{35}S]GTPγS trapped in the filters was determined by liquid scintillation counting. Pilot experiments were conducted to ensure that there is no depletion of ligand, nucleotides, and G proteins in the assay system.

Measurement of receptor thermal stability

A previously established method for determining receptor stability as a function of temperature in the absence of ligand was employed.[54,55] Approximately 5 μg of membrane preparations from the CB1 receptor-expressing HEK293 cells were incubated at the specified temperature for 30 min in the absence of ligand. Control samples for each receptor were kept on ice for 30 min. For every mutant, the different membrane aliquots were each heated at a single temperature ranging from 30°C to 100°C. After incubation, the samples were quenched on ice, re-homogenized, and added to TME buffer containing a near-saturating concentration of [^{3}H]CP55940 (147.9 Ci/mmol, PerkinElmer Life Sciences, Boston, MA) for further incubation for 60 min at 30°C. The radiolabeled-ligand was used at a concentration 10-fold above K_d for each receptor as determined by saturation binding,[56] to minimize the impact of any possible affinity change due to heat treatment. Nonspecific binding was determined in the presence of 1 μ*M* unlabeled ligand. Reactions were terminated by filtration with a Brandel cell harvester through Whatman GF/C filter paper. Radioactivity was measured by liquid scintillation counting. Three independent thermal stability measurements were carried out each in duplicate. The data were analyzed by non-linear regression using GraphPad Prism Software (GraphPad Software Inc., San Diego, CA) to obtain the slope and midpoint (apparent T_m) at 50% loss of specific binding as described previously.[54,55]

Radioligand binding assay

Saturation binding assays were performed as previously described.[56] Briefly, approximately 5 μg of membranes were incubated at 30°C for 60 min with [^{3}H]CP55940 (147.9 Ci/mmol, PerkinElmer Life Sciences, Boston, MA) or [^{3}H]SR141716A (43 Ci/mmol, PerkinElmer Life Sciences, Boston, MA) in a total volume of 200 μL or 500 μL TME buffer (25 m*M* Tris-HCl, 5m*M* $MgCl_2$, and 1 m*M* EDTA, pH 7.4) containing 0.1% fatty acid-free bovine

serum albumin. At least nine radiolabeled-ligand concentrations were used to determine K_d values of the receptors. Nonspecific binding was determined in the presence of 1 μM of unlabeled ligand. Reactions were terminated by filtration with a Brandel cell harvester through Whatman GF/C filter paper followed by four washes with ice-cold TME buffer to remove unbound radioactivity. Radioactivity was measured by liquid scintillation counting.

Data analysis

All data points represent the mean ± SE of at least three independent experiments performed in duplicate. For saturation radioligand binding assay, the K_d and B_{max} values were calculated by nonlinear regression using GraphPad Prism Software (GraphPad Software Inc., San Diego, CA). The values for the wild-type and mutant receptors were compared using analysis of variance (ANOVA) followed by Bonferroni's post hoc test for significance. P values of <0.05 were considered to be statistically significant.

RESULTS

Predicting interactions key to CB1 receptor activation

We previously demonstrated experimentally that the amino acids at position T3.46 and L3.43 are key to receptor activation.[10,11] Mutating T3.46 to isoleucine or L3.43 to alanine yielded highly constitutively active receptors, while replacing T3.46 with alanine inactivated the constitutively active wild-type CB1 receptor. To identify a structural basis for these experimental results, we predicted the ensemble of energetically favorable conformations for the wild-type, L3.43A, T3.46I, and T3.46A receptors using the first-principles-based GEnSeMBLE method.[22] Figure 1(A) shows the predicted structures of these receptors in terms of the key salt-bridges. We also found some differences in aromatic residue interactions and in hydrogen bonding interactions, however, we consider these changes to be less important in explaining the dramatic change from inactive to active structures.

The wild-type CB1 receptor is unique from other GPCRs because it has a threonine residue (T3.46) one turn above the conserved R3.50. In other GPCRs, this residue is either an alanine or a leucine. Our computational predictions indicate that CB1 contains a unique hydrogen bond involving T3.46 and S2.45. The S2.45 residue usually participates in the highly conserved 2-3-4 hydrogen bond network as observed in other crystallized GPCRs. By mutating T3.46 to alanine or leucine, we break this hydrogen bond connecting TM2 and 3, as seen in Figure 1(A.2). In the T3.46I mutant, the larger hydrophobic isoleucine side-chain pushes the surrounding helices, including TM6, away in order to provide enough room to avoid side-chain clashes. In the T3.46A mutant, the alanine residue is smaller than threonine and can fit in-between TMs 2 and 6. These two helices do not have to be as far away to avoid clashes as they would in the wild-type or T3.46I receptors. The T3.46A residue, however, does not interact with S2.45, so TM2 is rotated to optimize other polar interactions. In the L3.43A mutant, the threonine residue is left intact and thus so is the S2.45 and T3.46 hydrogen bond. The position of TM6 in relation to TM3 can change because the new alanine residue takes up less space than the original leucine one. The residues in the middle of TM6, such as V6.43, would clash with the 3.43 residue if the WT sequence had the L3.43A mutant

conformation. In the L3.43A mutant, the extracellular end tilts towards TM3, but the intracellular end moves away breaking the R3.50 + D6.30 interaction.

A comparison of the Cα-RMSD measure for the TM region across three of the functionally distinct structures, WT, T3.46A, and T3.46I, shows it to be 2.54 Å for the WT-T3.46A pair, 2.12 Å for the WT-T3.46I pair, and 2.86 Å for the T3.46A-T3.46I pair. A comparison of these numbers for the GPCRs crystallized in at least two distinct conformations was done. This Cα-RMSD measure for the common TM region for human β2 adrenergic receptor in the inactive (PDB ID: 2RH1) and the active (PDB ID: 3SN6) forms is: 2.48 Å. This measure for rhodopsin (PDB ID: 1U19) and metarhodopsin II (PDB ID: 3PQR) is 2.34 Å. For the adenosine A_{2A} receptor, the partially active form (PDB ID: 3QAK) deviates from the inactive form (PDB ID: 3EML) by 1.61 Å. The observed structural changes in the CB1 receptor in different functional forms are comparable in magnitude with that observed in the crystallized GPCRs. The smaller inactive-to-active deviation in the A_{2A} receptor is a manifestation of the fact that the active receptor is only partially active and cannot yet accommodate a G protein.

Comparing the predicted conformations for T3.46A, wild-type, T3.46I, and L3.43A, we found excellent correlation of the salt-bridge patterns with the experimentally determined extent of receptor activation (e.g. inactive, partially and fully active receptors) as summarized in Figure 1(B). We found that (1) only the fully inactive receptor has an R2.37 + D6.30 salt-bridge; note, the salt-bridge and hydrogen bond interactions are indicated by a plus (+) and a dash (–), respectively, throughout the text. (2) The weakly active wild-type receptor has R3.50 + D6.30 and D3.49 + K4.41 salt-bridges in addition to a D2.63 + K3.28 salt-bridge. (3) The highly constitutively active T3.46I and L3.43A receptors have neither of the R3.50 + D6.30 and D3.49 + K4.41 salt-bridges but both retain the D2.63 + K3.28 salt-bridge. Our interpretation of these results is that the presence of the R2.37 + D6.30 salt-bridge leads to a complete loss of activity even if the R3.50 + D6.30 and D3.49 + K4.41 salt-bridges are also present (as they are in T3.46A). At the other end of the spectrum, the D2.63 + K3.28 salt-bridge is required for full receptor activity (as in L3.43A and T3.46I) and it may be accompanied by a R5.71 + D6.30 salt-bridge (found in T3.46I) but this is not necessary for activation. However, when the D2.63 + K3.28 salt-bridge is accompanied by the R3.50 + D6.30 and D3.49 + K4.41 salt-bridges, they constrain the receptor to a less active state, and thus although the wild-type receptor also has this salt-bridge, it is only weakly active. These interpretations are consistent with the occurrence of this R3.50 + D6.30 salt-bridge between the DRY motif in TM3 and the D/E residue on the cytoplasmic side of TM6 in many GPCRs believed to be important for stabilizing the receptor inactive conformation.[57,58]

To evaluate the significance of these non-covalent interactions in receptor activation, we proceeded to predict a series of receptors with single and double point mutations which by the above concepts were expected to have specific changes in their activity and then experimentally tested their biochemical properties. The predicted structures highlighting the amino acids mutated, the R2.37 and D2.63 residues in TM2 and the L3.43 and T3.46 in TM3, are shown in Figure 2(A). Figure 2(B) illustrates the computationally predicted pattern of salt-bridges (R2.37 + D6.30, R3.50 + D6.30, D3.49 + K4.41, R5.71 + D6.30, and D2.63 +

K3.28) for the wild-type and some of CB1 mutant receptors. In addition to the highly active T3.46I and L3.43A and fully inactive T3.46A receptors analyzed previously,[10,11] we combined mutations that individually lead to constitutively active or inactive receptors (L3.43A, T3.46I, or T3.46A) with amino acid substitutions (R2.37A, R2.37Q, D2.63A) that break potential ionic interactions, R2.37 + D6.30 or D2.63 + K3.28. These include the R2.37Q/T3.46A, R2.37A/T3.46A, and D2.63A/L3.43A receptors. Given the pattern of salt-bridges identified in the consensus structures, these receptors are grouped by their expected levels of constitutive activity (e.g. highly active, partially active, or inactive). Figure 2(C) shows a full list of the CB1 receptors generated in this study in terms of predicted extent of constitutive activity. These include the L3.43A/T3.46I, L3.43A/T3.46A, and R2.37A/D2.63A/L3.43A receptors in addition to the receptors shown in Figure 2(B). We expect the L3.43A/T3.46I receptor to display a level of constitutive activity comparable to or higher than that of the L3.43A or the T3.46I receptor alone, since the individual mutations both lead to high constitutive activity. In contrast, the L3.43A/T3.46A mutant receptor is expected to possess somewhat reduced constitutive activity relative to the L3.43A mutation alone since it is combined with the inactivating alanine substitution at position T3.46.[10] Since our structure prediction indicates the salt-bridge between R2.37 and D6.30 is critical for maintaining the T3.46A receptor inactive, we expect that two mutant receptors, R2.37A/T3.46A and R2.37Q/T3.46A, will break the salt-bridge between R2.37 and D6.30. The D2.63A/L3.43A receptor was also constructed and cannot form the activating D2.63 + K3.28 salt-bridge. Interestingly, computational analysis indicates that this mutant receptor adopts the inactivating R2.37 + D6.30 salt-bridge. Thus, we expect breaking the resulting R2.37 + D6.30 salt-bridge in the D2.63A/L3.43A receptor would result in regaining of some constitutive activity. This is further tested by characterizing the triple mutant, R2.37A/D2.63A/L3.43A. Collectively, we hypothesized that the R2.37 + D6.30 and D2.63 + K3.28 salt-bridges may be critical for inactive and constitutively active conformations, respectively; however, if the latter is accompanied by a D3.49 + K4.41 and/or a R3.50 + D6.30 salt-bridge, like the wild-type, full receptor activity cannot be obtained. Some residues identified in Figure 1(B) (D3.49 and D6.30) have been excluded from this mutational study because they appear to be involved in multiple interactions making it difficult to interpret the data. Moreover, our predictions and others[57,59,60] suggested that they (as well as K3.28 and K4.41) may have a secondary role in receptor assembly and/or ligand interactions in addition to activation. The R5.71 + D6.30 salt-bridge has also been omitted in this study because this is present in the T3.46I receptor, but not in the L3.43A receptor, suggesting this interaction is not essential for receptor activation. The resulting mutant receptors were then evaluated for their biochemical properties to ascertain the extent to which receptor activity could be correlated with the non-covalent interactions identified.

Basal [^{35}S]GTPγS binding reveals the level of constitutive activity of the CB1 receptors

To measure directly the functional activity of the receptors, we investigated [^{35}S]GTPγS binding to HEK293 membranes expressing the CB1 wild-type and mutant receptors. The CB1 receptor is known to couple to pertussis toxin sensitive inhibitory G ($G_{i/o}$) protein. Thus, the [^{35}S]GTPγS binding assay is suitable for evaluating the G protein association with this receptor,[61] For basal G protein coupling activity, we measured [^{35}S]GTPγS binding to the membranes expressing the CB1 receptors in the absence of ligand. The level of GTPγS

binding for the T3.46A and D2.63A/L3.43A receptors is 53.2 fmol/mg and 53.3 fmol/mg, respectively, which is comparable to the level of a mock-transfected sample (53.2 fmol/mg) [Fig. 3(A)]. Thus, the residual activity observed by us (~ 53 fmol/mg) and others[62,63] is non-CB1 mediated and those receptors are in the fully inactive state. Two double mutants, the R2.37Q/T3.46A and R2.37A/T3.46A receptors, regained some constitutive activity, evidenced by the level of GTPγS binding of 77.0 fmol/mg and 72.5 fmol/mg, respectively. Interestingly, the triple mutant R2.37A/D2.63A/L3.43A also exhibited some level of constitutive activity (68.1 fmol/mg). Although these two double mutants and triple mutant displayed less constitutive activity than the wild-type (98.5 fmol/mg), the level is nonetheless remarkable; the data suggest that the salt-bridge involving the arginine at position 2.37 may be critical for the inactive conformation and when this interaction breaks, some constitutive activity is regained. The levels of GTPγS binding are only marginally different between the L3.43A/T3.46A and wild-type receptors. The L3.43A and T3.46I, and L3.43A/T3.46I receptors displayed the greatest constitutive activity with a similar level of GTPγS binding (112.3 fmol/mg, 114.5 fmol/mg, and 121.5 fmol/mg, respectively). Taken together, the experimentally measured levels of basal activity for the CB1 mutant receptors agree exceedingly well with the computationally predicted patterns of ionic interactions [Figs. 2(C) and 3(A)].

CP55940-stimulated [^{35}S]GTPγS binding suggests the maximal level of possible G protein coupling

To further evaluate how agonists impact the activity of the receptors, we investigated the agonist-promoted [^{35}S]GTPγS binding to membranes expressing the CB1 receptors. Figure 3(B) shows the level of CP55940-induced [^{35}S]GTPγS binding. Interestingly, regardless of the wide range of constitutive activity (basal level) exhibited by each receptor, CP55940 induced a similar level of GTPγS binding, suggesting this ligand may induce a comparable conformation for all the receptors examined with two exceptions (the D2.63A/L3.43A and T3.46A receptors). It is important to note that 1 μM CP55940 treatment induced little to no increase of GTPγS binding relative to the basal level for the L3.43A, T3.46I, and L3.43A/T3.46I receptors, suggesting these receptors may already adopt an active conformation comparable to a fully active receptor even in the absence of agonists. Intriguingly, although two inactive mutant receptors, D2.63A/L3.43A and T3.46A displayed a significant increase in GTPγS binding with 1 μ*M* CP55940, the levels were significantly lower than that of the wild-type [Fig. 3(B)]. This suggests that these inactive mutants are not able to be fully activated either because of a lack of particular non-covalent interactions critical for full receptor activation or because of the existence of a remaining constraint such as the TM2 + TM6 or TM3 + TM6 coupling that stabilizes the inactive state even upon CP55940 binding. Although the R2.37A/D2.63A/L3.43A receptor regained some constitutive activity in the absence of ligand, it was not fully activated by CP55940 suggesting the important role of the D2.63 residue in full receptor activation. Note that CP55940 treatment showed no change in the mock-transfected sample indicating that the CP55940-induced [^{35}S]GTPγS is CB1 receptor-mediated.

Thermal stabilities of the CB1 receptors are consistent with a spectrum of active states

It is generally accepted that the active conformation in its apo form is less stable relative to the inactive conformation.[64] Indeed, CAMs of many GPCRs have been shown to adopt the conformation having increased flexibility with marked instability.[64,65] To obtain an experimental measurement of the relative stability of the CB1 receptors, we preformed thermal denaturation assays in the absence of ligand as previously established by many groups.[54,55] The term “stability” used in this study is defined as the ability of the receptor to maintain a correctly folded state, especially within its binding pocket believed to form within the helical bundle. Since the wild-type receptor has been shown to possess significant constitutive activity,[18,66] it can become either inactive or fully active, and consequently its temperature midpoint of the denaturation curve, $T_{m,}$ should vary accordingly with the mutations described. As shown in Figure 4(A) and Table I, the thermal denaturation for the L3.43A/T3.46I receptor leads to the lowest T_m of 55.8 ± 1.2° for the series followed by the L3.43A and T3.46I receptors with 57.2 ± 1.6°C and 58.1 ± 0.5°C, respectively. The difference in T_m values between the L3.43A and T3.46I receptors is not statistically significant. The L3.43A/T3.46A receptor also exhibits substantially less stability (T_m = 60.7 ± 1.1°C) relative to the wild-type receptor, which denatures with a T_m = 64.5 ± 1.1°C. Consistent with the trend observed from basal GTPγS binding data, two receptors with double substitutions, R2.37Q/T3.46A and R2.37A/T3.46A, and the triple mutant receptor R2.37A/D2.63A/L3.43A showed enhanced thermal stability relative to the wild-type receptor with T_m values of 67.2 ± 1.0°C, 68.1 ± 0.9°C, and 69.8 ± 1.2°C, respectively [Fig. 4(B) and Table I]. Our data also indicates that the inactive receptors, T3.46A and D2.63A/L3.43A, adopted the most stable conformation among the receptors we tested, indicated by their T_m (71.4 ± 1.8°C and 72.1 ± 2.1°C, respectively). Taken together with the basal G protein coupling data, we demonstrate that in the absence of ligand, the single and double mutations on TM2 and TM3 progressively impact the receptor's thermal stability correlating well with predicted conformational changes, and in turn changes in the equilibrium between the inactive (R) and highly active receptor (R*). Figure 4(C) shows an excellent correlation between the T_m and the receptor activity level determined from GTPγS binding with an R^2 value of 0.9722. This indicates that the conformational change adopted by these mutants results in a corresponding functional change, as the receptor becomes thermodynamically less stable with increasing activity.

Ligand binding affinity reflects extent of basal activity

One of the remarkable characteristics of CAMs is that their ligand binding affinity shifts due to pre-coupling to the G protein. In general, CAMs are characterized by enhanced affinity for agonists and decreased affinity for inverse agonists, whereas inactive GPCRs exhibit the opposite characteristics; decreased affinity for agonists and enhanced affinity for inverse agonist.[6,39,40] To evaluate the predicted correlations between the key intramolecular interactions of the receptor with ligand binding profiles and consequently test the predictions of the extended ternary complex model on the series of mutant receptors shown in Figure 2(B), we carried out saturation binding experiments using the CB1 agonist [^{3}H]CP55940 and the inverse agonist [^{3}H]SR141716A. In agreement with ligand binding properties for other GPCR CAMs,[6,39,40] saturation binding analysis indicates the T3.46I and L3.43A receptors display an improved affinity for CP55940 by sixfold with K_d values of 0.31 ± 0.04

n*M* and 0.32 ± 0.13 nM, respectively, relative to the wild-type receptor (K_d of 1.78 ± 0.32 n*M*) (Table II). The inactive mutant receptor T3.46A displays a sixfold reduced affinity for CP55940 compared to the wild-type receptor with a K_d value of 9.83 ± 1.12 n*M*. This is consistent with our previous homologous competition binding data for these receptors.[10,11]

As predicted, the L3.43A/T3.46I receptor exhibits a K_d value (0.28 ± 0.02 n*M*) comparable to the individual single mutant receptors, L3.43A and T3.46I, whereas the L3.43A/T3.46A showed a wild-type-like affinity for CP55940 with K_d of 1.10 ± 0.23 n*M*.

Since the salt-bridge between R2.37 and D6.30 cannot form in the R2.37A/T3.46A, R2.37Q/T3.46A, and R2.37A/D2.63A/L3.43A receptors, these receptors exhibited ligand binding affinity profiles between those of the T3.46A and wild-type receptors with K_d values of 5.58 ± 0.32 n*M*, 6.21 ± 1.11 n*M*, and 7.63 ± 0.89, respectively, confirming that the R2.37 is critical for the CB1 inactive conformation.

In order to evaluate the importance of D2.63 on the transition to an active conformation, we considered the D2.63A/L3.43A mutant, which was predicted to be inactive. Indeed, this mutant receptor showed a markedly decreased affinity for CP55940 with a K_d of 12.74 ± 2.13 n*M*, which is comparable to the inactive T3.46A receptor, confirming the theoretical prediction that D2.63 is required for activation of this receptor. No significant differences were observed between the B_{max} values of any of the mutant receptors tested.

In accordance with the extended ternary complex model,[3] agonists shift the equilibrium toward a state where active receptors (R*) predominate, whereas inverse agonists increase the inactive receptor (R) population. Therefore, this model predicts that constitutively active receptors possess increased affinity for agonist, as we demonstrated with CP55940. The affinity changes of CB1 receptors with single and double mutations for the agonist CP55940 inspired us to also assess the effect of the mutations on the affinity for inverse agonist using [^{3}H]SR141716A. The saturation binding parameters for [^{3}H]SR141716A for the CB1 mutant receptors along with the wild-type receptor are shown in Table II. Interestingly, the overall rank order of affinity for [^{3}H]SR141716A was opposite to that for [^{3}H]CP55940. For example, the D2.63A/L3.43A (0.64 ± 0.07 n*M*) and T3.46A (0.61 ± 0.09 n*M*) receptors exhibited threefold greater affinity than the wild-type (2.11 ± 0.42 n*M*) for [^{3}H]SR141716A. The R2.37Q/T3.46A (1.59 ± 0.22 n*M*), R2.37A/T3.46A (1.67 ± 0.26 nM), and R2.37A/D2.63A/L3.43A (1.48 ± 0.20) receptors showed slightly lower but not statistically significant K_d values for inverse agonist binding relative to the wild-type receptor. The L3.43A/T3.46A receptor exhibited a fourfold lower affinity with a K_d value of 7.50 ± 0.46 n*M*. Two single mutants, L3.43A and T3.46I, and a double mutant L3.43A/T3.46I displayed a sevenfold and sixfold lower affinity, respectively, than the wild-type receptor. All mutant receptors showed negligible B_{max} changes in [^{3}H]SR141716A binding, showing similar expression levels among the receptors tested in this study. Taken together, shifts in affinity for [^{3}H]CP55940 and [^{3}H]SR141716A suggest that the mutant receptors exist in different and graded states of receptor activation in the absence of ligand, consistent with the extended ternary complex model.[3] This is especially apparent if the K_d ratios for each mutant and wild-type receptors are compared (Table II). Thus, the GTPγS data, thermal stability, and ligand binding properties demonstrate that the single and double mutations on

TM2 and TM3 impact the receptor's functional activity, providing an array of constitutive activity from the inactive (R) to highly active receptor states (R*).

DISCUSSION

A central question driving GPCR structural studies involves how the individual TMs move and interact during activation and how this rearrangement affects their interactions with downstream signaling molecules, such as G-proteins, β-arrestins, and G-protein coupled receptor kinases. To address this fundamental question, we predicted the CB1 receptor structures for the wild-type and several mutants and found systematic differences of specific inter-helical interactions critical to different levels of receptor activation. We observed shifts in G-protein coupling activity, receptor stability, and ligand binding affinity consistent with our computational predictions. Consequently, we have generated a collection of CB1 receptors involving minimal modifications that collectively exhibit a continuum of constitutive activity. These include two mutant receptors, D2.63A/L3.43A and T3.46A, that we predicted would be inactive and which subsequent experiments, indeed, showed to display inactive receptor properties. These involved mutations that lead to functions opposite of those exhibited by CAMs. The properties of the D2.63A/L3.43A receptor are particularly remarkable because computational analysis indicates that it adopts the inactivating R2.37 + D6.30 salt-bridge while experiments show the profiles corresponding to an inactive receptor (Table II); this mutant receptor cannot form the D2.63 + K3.28 activating salt-bridge and thus is inactive despite the inclusion of the L3.43A mutation. It is important to note that we included only one residue of each of the two salt bridges (e.g. D2.63 and R2.37) for mutational study, since each respective partners (D6.30 and K3.28, respectively) is likely involved in multiple interactions critical for receptor activation and ligand binding.[59,60,67,68] Therefore, our mutational study does not firmly rule out the possibility that the salt-bridges did not involve the D6.30 and K3.28 residues. However, the computationally predicted formation of the R2.37 + D6.30 salt-bridge in the D2.63A/L3.43A receptor was tested by the triple mutant, D2.63A/L3.43A/R2.37A (Figs. 3 and 4, Tables I and II), and the data further support that the R2.37 residue is critical for receptor activity likely through interaction with D6.30. We predict that a similar salt-bridge pattern can be achieved for more than a single CAM. For example, we demonstrated that both T3.46I and L3.43A are highly constitutively active and share key salt-bridge interactions, such as the D2.63 + K3.28 [Fig. 1(B)]. Similarly, two inactive mutants T3.46A and D2.63A/L3.43A retained the TM2 + TM6 lock. Thus, our proposed activation mechanism reveals key global interactions responsible for receptor activation rather than specific local interaction changes. Given that GPCRs can adopt multiple activation states, our activation mechanism provides a structural template that can be expanded further to test for other CAMs. Since the first CAM was generated for the α_{1B}-adrenergic receptor leading to spontaneous G-protein activation in the absence of an agonist,[6,69] single amino acid substitutions in various regions of different GPCRs have been shown to produce enhanced constitutive activity.[70,71] These regions include the cytoplasmic extensions of TMs 2, 3, 6, and 7, indicating that these are sensitive to receptor activity. Intriguingly, recent studies demonstrate that mutations on the extracellular loops 2 and 3 can also result in enhanced constitutive activity in the C5a and adenosine A2b receptors.[72,73] Molecular modeling data suggest that some mutations on the extracellular loops alter the

interactions between the loops and TMs, which in turn impact the TM helix packing arrangement involving TMs 2, 3, and 7.[72] In addition to the crystal structures of inactive GPCRs, a few GPCRs have been recently crystallized in the active conformation including rhodopsin, the β_2-adrenergic receptor and the A_{2A} adenosine receptor.[25,74–77] These active state structures reveal some common patterns of conformational changes providing snapshots of the "active" forms. For example, metarhodopsin II, Gs-bound β2-adrenergic receptors, and the A_{2A} adenosine receptor displayed significant conformational changes due to alteration of the inter-helical hydrogen bond network involving residues in TMs 3, 5, 6 and 7 near the ligand binding pocket.[75,77,78] This suggests that although the residues interacting with agonists are largely receptor specific, they seem to undergo a similar conformational change via these TMs upon activation. A similar pattern of TM movement upon activation was observed in our predicted CB1 structures.[23] In addition, the "active" forms exhibit a rearrangement (tilting and rotation) of TM6 and neutralization of D3.49 in the DRY motif of TM3. Those adjustments allow for accommodation of the G-protein at the cytoplasmic side of the receptors.[25,74,76,77] Our predicted receptor conformations are consistent with this, indicating that CB1 also undergoes a similar activation mechanism involving TM6 and TM3. However, our data also indicate the existence of a TM2 + TM6 salt-bridge in the inactive conformation, which is unique to the CB1 receptor and points to an additional element in its mechanism of activation. Breaking the R2.37 + D6.30 and forming the D2.63 + K3.28 salt-bridge are critical for constitutive activity.

In addition to disruption of key salt-bridges,[79,80] our paradigm for GPCR activation involves rigid body movement of the TMs due to changes in the hydrogen bonding network[81,82] and aromatic residue interactions.[83,84] For example, our predicted structures contain multiple hydrogen bonds involving TM2 and TM4 that have also been found in the crystallized GPCRs.[21,25,85-87] We predict a H2.41-K4.41 hydrogen bond in the wild-type receptor and a Y2.40-R4.39 hydrogen bond in both wild-type and T3.46I mutant receptors. A Y2.41-K4.43 hydrogen bond has been observed experimentally in the inactive human A2A adenosine receptor structure,[85] and a Y2.41-E4.39 hydrogen bond has been observed in multiple crystal structures including bovine rhodopsin,[21] the active opsin,[86,87] and the active meta II.[25] However, since the presence of these non-covalent interactions varies among different receptor states, our computational predictions strongly suggest that intracellular ionic interactions are the driving force leading to the dramatic changes in activity among the receptors we tested. This is consistent with MD simulations on the β2 adrenergic receptor.[88]

It is well accepted that high constitutive activity requires the absence of intramolecular interactions that constrain the receptor in the R state.[89] Our proposed helix packing pattern shows that the highly constitutively active mutant receptors, L3.43A/T3.46I, L3.43A, and T3.46I lack the intracellular ionic coupling across TMs, such as the most conserved TM3 + TM6 ionic lock and the TM2 + TM6 salt-bridge are present in the inactive form of CB1. Instead, the active receptors seem to possess salt-bridge interactions between neighboring TMs (e.g. TM2 + TM3 and TM5 + TM6) resulting in a larger diameter (11.64 Å) at the cytoplasmic end of TM3 and TM6 than that of the T3.46A (8.47 Å) or wild-type (8.93 Å) receptors. This conformational change may facilitate accommodation of the C-terminal α-helix of the G_α protein during receptor activation.[87] The lack of the constraining salt-bridges that are present in the inactive mutants and slightly active wild-type receptor allows the

CAM receptors to relax into the R* conformation and the transition to this conformation results in enhanced conformational flexibility and lower stability. To measure the structural stability of GPCRs, a thermal stability measurement was developed for GPCRs by many groups.[55,64] Initially, GPCR thermal stability was measured to screen for more stable conformations for structural analysis such as X-ray crystallography.[90,91] We applied these measurements to each receptor to evaluate the correlation between receptor activity and conformational instability in the absence of ligand during the denaturing step (heat treatment) at various temperatures and subsequently determined the stability by quantitative measurement of the loss of ligand binding ability as described previously.[54,55] Our data demonstrate that the more active conformations are less stable and denature at lower temperatures (the apparent T_m). In addition, the good correlation between receptor stability and activity, and the pattern of agonist and inverse agonist affinity for each receptor suggests that the stability change observed is not merely due to the point mutation per se. Rather it is due to global conformational changes involving multiple TMs (TMs 2, 3, 5, and 6) stemming from differential salt-bridge patterns. This is consistent with the predicted structures for those receptors with mutations in TMs 2 and 3. The observation that the inactive single mutant T3.46A is much more stable than the wild-type receptor strongly indicates that structural changes resulting from this single mutation are sufficiently substantial to provide enhanced stability of the mutant receptor; this is consistent with the changes observed in the predicted structures.

Intriguingly, although two inactive mutant receptors, D2.63A/L3.43A and T3.46A displayed a significant increase in GTPγS binding with 1 μ*M* CP55940 treatment, the levels were substantially lower than that of the wild-type [Fig. 3(B)]. This may suggest that these inactive mutants can only partially mimic the activated conformations upon agonist binding. Perhaps ligand-induced full activation is not possible due to their lack of interactions critical for full receptor activation or else the existence of remaining constraints that stabilize the inactive state even upon CP55940 binding. Moreover, treatment with even higher concentrations of CP55940 (10 μ*M*) failed to show any further increase in GTPγS binding (data not shown), suggesting that reduced affinity of the agonist for those receptors is not the underlying cause of the partial increase of CP55940-induced GTPγS binding observed. In contrast, all other constitutively active receptors (L3.43A/T3.46I, T3.46I, L3.43A, L3.43A/T3.46A, wild-type, R2.37Q/T3.46A, and R2.37A/T3.46A) exhibited a similar level of maximum GTPγS binding with 1 μ*M* CP55940 treatment. This data suggest that CP55940 induces a comparable conformation in the highly active mutant receptors (T3.46I and L3.43A). It would be interesting to further investigate how CP55940 docking alters the key salt-bridge pattern using the mutant receptors possessing different levels of constitutive activity.

In addition to experimentally testing structural predictions, this study permitted experimental testing of the extended ternary complex and related models with respect to agonist and inverse agonist affinity shifts.[2,92,93] Using the wide activity range of CB1 receptors evaluated here, we have for the first time demonstrated that the activity hierarchy of these receptors is consistent with their ligand binding profile: the highly constitutive active receptor exhibits an increased affinity for agonist but decreased affinity for inverse agonist; the fully inactive receptor exhibits the reverse; and the partially active receptors display

intermediate profiles. These CB1 receptors provide a powerful framework for understanding the molecular basis for the multiple stages of receptor activation. These receptors also provide a good tool to screen for novel inverse agonists or partial agonists, which can selectively target receptors at different levels of activation.

Acknowledgments

Grant sponsor: National Institutes of Health; Grant number: DA020763 (to D.A.K), NS071112, NS073115, AI040567 (to W.A.G.)

Abbreviations

BSA	bovine serum albumin
CAM	constitutively active mutant
CB1	cannabinoid 1 receptor
CP55940	(1*R*,3*R*,4*R*)-3-[2-hydroxy-4-(1,1-dimethylheptyl)-phenyl]-4-(3-hydroxypropyl)cyclohexan-1-ol
GEnSeMBLE MC	GPCR Ensemble of Structures in Membrane Bilayer Environment Monte Carlo
GPCR	G-protein coupled receptor
GTPγS	guanosine 5′-*O*-(3-thiotriphosophate)
HEK	human embryonic kidney cell
PBS	phosphate-buffered saline
SR141716A	*N*-(piperidin-1-yl)-5-(4-chlorophenyl)-1-(2,4-dichlorophenyl)-4-methyl-1*H*-pyrazole-3-carboxamide
T_m	temperature midpoint of denaturation curve
TM	transmembrane
TME	Tris/Mg^{2+}EDTA

REFERENCES

1. Howlett AC, Barth F, Bonner TI, Cabral G, Casellas P, Devane WA, Felder CC, Herkenham M, Mackie K, Martin BR, Mechoulam R, Pertwee RG. International Union of Pharmacology. XXVII. Classification of cannabinoid receptors. Pharmacol Rev. 2002; 54:161–202. [PubMed: 12037135]
2. De Lean A, Stadel JM, Lefkowitz RJ. A ternary complex model explains the agonist-specific binding properties of the adenylate cyclase-coupled beta-adrenergic receptor. J Biol Chem. 1980; 255:7108–7117. [PubMed: 6248546]
3. Samama P, Cotecchia S, Costa T, Lefkowitz RJ. A mutation-induced activated state of the beta 2-adrenergic receptor. Extending the ternary complex model. J Biol Chem. 1993; 268:4625–4636. [PubMed: 8095262]
4. Chidiac P, Hebert TE, Valiquette M, Dennis M, Bouvier M. Inverse agonist activity of beta-adrenergic antagonists. Mol Pharmacol. 1994; 45:490–499. [PubMed: 7908406]
5. Govardhan CP, Oprian DD. Active site-directed inactivation of constitutively active mutants of rhodopsin. J Biol Chem. 1994; 269:6524–6527. [PubMed: 8120004]

6. Cotecchia S, Exum S, Caron MG, Lefkowitz RJ. Regions of the alpha 1-adrenergic receptor involved in coupling to phosphatidylinositol hydrolysis and enhanced sensitivity of biological function. Proc Natl Acad Sci USA. 1990; 87:2896–2900. [PubMed: 2158097]

7. Bakker RA, Jongejan A, Sansuk K, Hacksell U, Timmerman H, Brann MR, Weiner DM, Pardo L, Leurs R. Constitutively active mutants of the histamine H1 receptor suggest a conserved hydrophobic asparagine-cage that constrains the activation of class A G protein-coupled receptors. Mol Pharmacol. 2008; 73:94–103. [PubMed: 17959710]

8. Boucard AA, Roy M, Beaulieu ME, Lavigne P, Escher E, Guillemette G, Leduc R. Constitutive activation of the angiotensin II type 1 receptor alters the spatial proximity of transmembrane 7 to the ligand-binding pocket. J Biol Chem. 2003; 278:36628–36636. [PubMed: 12842881]

9. Befort K, Zilliox C, Filliol D, Yue S, Kieffer BL. Constitutive activation of the delta opioid receptor by mutations in transmembrane domains III and VII. J Biol Chem. 1999; 274:18574–18581. [PubMed: 10373467]

10. D'Antona AM, Ahn KH, Kendall DA. Mutations of CB1 T210 produce active and inactive receptor forms: correlations with ligand affinity, receptor stability, and cellular localization. Biochemistry. 2006; 45:5606–5617. [PubMed: 16634642]

11. D'Antona AM, Ahn KH, Wang L, Mierke DF, Lucas-Lenard J, Kendall DA. A cannabinoid receptor 1 mutation proximal to the DRY motif results in constitutive activity and reveals intramolecular interactions involved in receptor activation. Brain Res. 2006; 1108:1–11. [PubMed: 16879811]

12. Kenakin T. Ligand-selective receptor conformations revisited: the promise and the problem. Trends Pharmacol Sci. 2003; 24:346–354. [PubMed: 12871667]

13. Niesen MJ, Bhattacharya S, Vaidehi N. The role of conformational ensembles in ligand recognition in G-protein coupled receptors. J Am Chem Soc. 2011; 133:13197–13204. [PubMed: 21766860]

14. Stallaert W, Christopoulos A, Bouvier M. Ligand functional selectivity and quantitative pharmacology at G protein-coupled receptors. Expert Opin Drug Discov. 2011; 6:811–825. [PubMed: 22651124]

15. Yao XJ, Velez Ruiz G, Whorton MR, Rasmussen SG, DeVree BT, Deupi X, Sunahara RK, Kobilka B. The effect of ligand efficacy on the formation and stability of a GPCR-G protein complex. Proc Natl Acad Sci USA. 2009; 106:9501–9506. [PubMed: 19470481]

16. Lefkowitz RJ, Cotecchia S, Samama P, Costa T. Constitutive activity of receptors coupled to guanine nucleotide regulatory proteins. Trends Pharmacol Sci. 1993; 14:303–307. [PubMed: 8249148]

17. Seifert R, Wenzel-Seifert K. Constitutive activity of G-protein-coupled receptors: cause of disease and common property of wild-type receptors. Naunyn Schmiedebergs Arch Pharmacol. 2002; 366:381–416. [PubMed: 12382069]

18. Bouaboula M, Perrachon S, Milligan L, Canat X, Rinaldi-Carmona M, Portier M, Barth F, Calandra B, Pecceu F, Lupker J, Maffrand JP, Le Fur G, Casellas P. A selective inverse agonist for central cannabinoid receptor inhibits mitogen-activated protein kinase activation stimulated by insulin or insulin-like growth factor 1. Evidence for a new model of receptor/ligand interactions. J Biol Chem. 1997; 272:22330–22339. [PubMed: 9268384]

19. Pertwee RG, Howlett AC, Abood ME, Alexander SP, Di Marzo V, Elphick MR, Greasley PJ, Hansen HS, Kunos G, Mackie K, Mechoulam R, Ross RA. International Union of Basic and Clinical Pharmacology. LXXIX. Cannabinoid receptors and their ligands: beyond CB(1) and CB(2). Pharmacol Rev. 2010; 62:588–631. [PubMed: 21079038]

20. Ballesteros, JA.; Weinstein, H. Integrated methods for the construction of three-dimensional models and computational probing of structure-function relations in G protein-coupled receptors.. In: Stuart, CS., editor. Methods in neurosciences. Vol. 25. Academic Press; San Diego, CA: 1995. p. 366-428.

21. Palczewski K, Kumasaka T, Hori T, Behnke CA, Motoshima H, Fox BA, Le Trong I, Teller DC, Okada T, Stenkamp RE, Yamamoto M, Miyano M. Crystal structure of rhodopsin: a G protein-coupled receptor. Science. 2000; 289:739–745. [PubMed: 10926528]

22. Abrol, R.; Griffith, AR.; Bray, JK.; Goddard, WA, III.. Structure Prediction of G Protein-Coupled Receptors and Their Ensemble of Functionally Important Conformations.. In: Vaidehi, N.; Klein-

Seetharaman, J., editors. Methods in molecular biology “membrane protein structure: methods and protocols”. Vol. 914. Humana; New York: 2012.

23. Scott CE, Abrol R, Ahn KH, Kendall DA, Goddard WA III. Molecular basis for dramatic changes in cannabinoid CB1 G protein-coupled receptor activation upon single and double point mutations. Protein Sci. 2013; 22:101–113. [PubMed: 23184890]
24. Chien EYT, Liu W, Zhao QA, Katritch V, Han GW, Hanson MA, Shi L, Newman AH, Javitch JA, Cherezov V, Stevens RC. Structure of the human dopamine D3 receptor in complex with a D2/D3 selective antagonist. Science. 2010; 330:1091–1095. [PubMed: 21097933]
25. Choe HW, Kim YJ, Park JH, Morizumi T, Pai EF, Krauss N, Hof-mann KP, Scheerer P, Ernst OP. Crystal structure of metarhodopsin II. Nature. 2011; 471:651–655. [PubMed: 21389988]
26. Murakami M, Kouyama T. Crystal structure of squid rhodopsin. Nature. 2008; 453:363–367. [PubMed: 18480818]
27. Li J, Edwards PC, Burghammer M, Villa C, Schertler GFX. Structure of bovine rhodopsin in a trigonal crystal form. J Mol Biol. 2004; 343:1409–1438. [PubMed: 15491621]
28. Okada T, Fujiyoshi Y, Silow M, Navarro J, Landau EM, Shichida Y. Functional role of internal water molecules in rhodopsin revealed by x-ray crystallography. Proc Natl Acad Sci USA. 2002; 99:5982–5987. [PubMed: 11972040]
29. Okada T, Sugihara M, Bondar A-N, Elstner M, Entel P, Buss V. The retinal conformation and its environment in rhodopsin in light of a new 2.2 a crystal structure. J Mol Biol. 2004; 342:571–583. [PubMed: 15327956]
30. Salom D, Lodowski DT, Stenkamp RE, Le Trong I, Golczak M, Jastrzebska B, Harris T, Ballesteros JA, Palczewski K. Crystal structure of a photoactivated deprotonated intermediate of rhodopsin. Proc Natl Acad Sci USA. 2006; 103:16123–16128. [PubMed: 17060607]
31. Stenkamp RE. Alternative models for two crystal structures of bovine rhodopsin. Acta Crystallogr D Biol Crystallogr. 2008; 64:902–904. [PubMed: 18645239]
32. Teller DC, Okada T, Behnke CA, Palczewski K, Stenkamp RE. Advances in determination of a high-resolution three-dimensional structure of rhodopsin, a model of G-protein-coupled receptors (GPCRs). Biochemistry. 2001; 40:7761–7772. [PubMed: 11425302]
33. Doré AS, Robertson N, Errey JC, Ng I, Hollenstein K, Tehan B, Hurrell E, Bennett K, Congreve M, Magnani F, Tate CG, Weir M, Marshall FH. Structure of the adenosine A_{2A} receptor in complex with ZM241385 and the xanthines XAC and caffeine. Structure. 2011; 19:1283–1293. [PubMed: 21885291]
34. Rasmussen SGF, DeVree BT, Zou Y, Kruse AC, Chung KY, Kobilka TS, Thian FS, Chae PS, Pardon E, Calinski D, Mathiesen JM, Shah STA, Lyons JA, Caffrey M, Gellman SH, Steyaert J, Skiniotis G, Weis WI, Sunahara RK, Kobilka BK. Crystal structure of the b_2 adrenergic receptor-Gs protein complex. Nature. 2011; 477:549–555. [PubMed: 21772288]
35. Rasmussen SGF, Choi H-J, Fung JJ, Pardon E, Casarosa P, Chae PS, DeVree BT, Rosenbaum DM, Thian FS, Kobilka TS, Schnapp A, Konetzki I, Sunahara RK, Gellman SH, Pautsch A, Steyaert J, Weis WI, Kobilka BK. Structure of a nanobody-stabilized active state of the beta2 adrenoceptor. Nature. 2011; 469:175–180. [PubMed: 21228869]
36. Wu B, Chien EYT, Mol CD, Fenalti G, Liu W, Katritch V, Abagyan R, Brooun A, Wells P, Bi FC, Hamel DJ, Kuhn P, Handel TM, Cherezov V, Stevens RC. Structures of the CXCR4 chemokine GPCR with small-molecule and cyclic peptide antagonists. Science. 2010; 330:1066–1071. [PubMed: 20929726]
37. Park JH, Scheerer P, Hofmann KP, Choe H-W, Ernst OP. Crystal structure of the ligand-free G-protein-coupled receptor opsin. Nature. 2008; 454:183–187. [PubMed: 18563085]
38. Hanson MA, Roth CB, Jo E, Griffith MT, Scott FL, Reinhart G, Desale H, Clemons B, Cahalan SM, Schuerer SC, Sanna MG, Han GW, Kuhn P, Rosen H, Stevens RC. Crystal Structure of a lipid G protein-coupled receptor. Science. 2012; 335:851–855. [PubMed: 22344443]
39. McWhinney C, Wenham D, Kanwal S, Kalman V, Hansen C, Robishaw JD. Constitutively active mutants of the alpha(1a)- and the alpha(1b)-adrenergic receptor subtypes reveal coupling to different signaling pathways and physiological responses in rat cardiac myocytes. J Biol Chem. 2000; 275:2087–2097. [PubMed: 10636913]

40. Wade SM, Lan K, Moore DJ, Neubig RR. Inverse agonist activity at the alpha(2A)-adrenergic receptor. Mol Pharmacol. 2001; 59:532–542. [PubMed: 11179449]
41. Mayo SL, Olafson BD, Goddard WA. Dreiding—a generic force-field for molecular simulations. J Phys Chem. 1990; 94:8897–8909.
42. Wimley WC, White SH. Experimentally determined hydrophobicity scale for proteins at membrane interfaces. Nat Struct Biol. 1996; 3:842–848. [PubMed: 8836100]
43. Pollastri G, McLysaght A. Porter: a new, accurate server for protein secondary structure prediction. Bioinformatics. 2004; 21:1719–1720. [PubMed: 15585524]
44. Pollastri, G. Porter protein secondary structure prediction at University College Dublin. Dublin, Ireland: 2012. Available at: http://distill.ucd.ie/porter/
45. Raghava, GPS. APSSP2: A combination method for protein secondary structure prediction based on neural network and example based learning. CASP5; 2002. p. A-132.
46. Raghava, GPS. APSSP2: advanced protein secondary structure prediction server. Chandigarh, India: 2012. Available at: http://www.imtech.res.in/raghava/apssp2/
47. Jones DT. Protein secondary structure prediction based on position-specific scoring matrices. J Mol Biol. 1999; 292:195–202. [PubMed: 10493868]
48. Bryson K, McGuffin LJ, Marsden RL, Ward JJ, Sodhi JS, Jones DT. Protein structure prediction servers at university college london. Nucleic Acids Res. 2005; 33(Web server issue):W36–W38. [PubMed: 15980489]
49. Jones, DT.; Buchan, D.; Ward, S.; Lobley, A.; Nugent, T.; Bryson, K.; McGuffin, LJ. Group DDBB. , editor. UCL Department of Computer Science, London, UK.. The PSIPRED protein structure prediction server; 2002-2008. Available at:http://bioinf.cs.ucl.ac.uk/psipred/
50. Kam VWT, Goddard WA. Flat-bottom strategy for improved accuracy in protein side-chain placements. J Chem Theor Comput. 2008; 4:2160–2169.
51. Abrol R, Bray JK, Goddard WA III. Bihelix: Towards de novo structure prediction of an ensemble of G-protein coupled receptor conformations. Proteins. 2012; 80:505–518. [PubMed: 22173949]
52. Ahn KH, Bertalovitz AC, Mierke DF, Kendall DA. Dual role of the second extracellular loop of the cannabinoid receptor 1: ligand binding and receptor localization. Mol Pharmacol. 2009; 76:833–842. [PubMed: 19643997]
53. Chen C, Okayama H. High-efficiency transformation of mammalian cells by plasmid DNA. Mol Cell Biol. 1987; 7:2745–2752. [PubMed: 3670292]
54. Liu W, Hanson MA, Stevens RC, Cherezov V. LCP-Tm: an assay to measure and understand stability of membrane proteins in a membrane environment. Biophys J. 2010; 98:1539–1548. [PubMed: 20409473]
55. Magnani F, Shibata Y, Serrano-Vega MJ, Tate CG. Co-evolving stability and conformational homogeneity of the human adenosine A2a receptor. Proc Natl Acad Sci USA. 2008; 105:10744–10749. [PubMed: 18664584]
56. Ahn KH, Mahmoud MM, Kendall DA. Allosteric modulator ORG27569 induces CB1 cannabinoid receptor high affinity agonist binding state, receptor internalization, and Gi protein-independent ERK1/2 kinase activation. J Biol Chem. 2012; 287:12070–12082. [PubMed: 22343625]
57. Hurst DP, Lynch DL, Barnett-Norris J, Hyatt SM, Seltzman HH, Zhong M, Song ZH, Nie J, Lewis D, Reggio PH. N-(piperidin-1-yl)-5-(4-chlorophenyl)-1-(2,4-dichlorophenyl)-4-methyl-1H-pyrazole-3-carboxamide (SR141716A) interaction with LYS 3.28(192) is crucial for its inverse agonism at the cannabinoid CB1 receptor. Mol Pharmacol. 2002; 62:1274–1287. [PubMed: 12435794]
58. Li J, Edwards PC, Burghammer M, Villa C, Schertler GF. Structure of bovine rhodopsin in a trigonal crystal form. J Mol Biol. 2004; 343:1409–1438. [PubMed: 15491621]
59. Salo OM, Lahtela-Kakkonen M, Gynther J, Jarvinen T, Poso A. Development of a 3D model for the human cannabinoid CB1 receptor. J Med Chem. 2004; 47:3048–3057. [PubMed: 15163186]
60. Shim JY, Howlett AC. WIN55212-2 docking to the CB1 cannabinoid receptor and multiple pathways for conformational induction. J Chem Inf Model. 2006; 46:1286–1300. [PubMed: 16711748]
61. Harrison C, Traynor JR. The [35S]GTPgammaS binding assay: approaches and applications in pharmacology. Life Sci. 2003; 74:489–508. [PubMed: 14609727]

62. Kapur A, Samaniego P, Thakur GA, Makriyannis A, Abood ME. Mapping the structural requirements in the CB1 cannabinoid receptor transmembrane helix II for signal transduction. J Pharmacol Exp Ther. 2008; 325:341–348. [PubMed: 18174385]

63. McAllister SD, Hurst DP, Barnett-Norris J, Lynch D, Reggio PH, Abood ME. Structural mimicry in class A G protein-coupled receptor rotamer toggle switches: the importance of the F3.36(201)/W6.48(357) interaction in cannabinoid CB1 receptor activation. J Biol Chem. 2004; 279:48024–48037. [PubMed: 15326174]

64. Gether U, Ballesteros JA, Seifert R, Sanders-Bush E, Weinstein H, Kobilka BK. Structural instability of a constitutively active G protein-coupled receptor. Agonist-independent activation due to conformational flexibility. J Biol Chem. 1997; 272:2587–2590. [PubMed: 9006889]

65. Samama P, Bond RA, Rockman HA, Milano CA, Lefkowitz RJ. Ligand-induced overexpression of a constitutively active beta2-adrenergic receptor: pharmacological creation of a phenotype in transgenic mice. Proc Natl Acad Sci USA. 1997; 94:137–141. [PubMed: 8990174]

66. Fioravanti B, De Felice M, Stucky CL, Medler KA, Luo MC, Gardell LR, Ibrahim M, Malan TP Jr. Yamamura HI, Ossipov MH, King T, Lai J, Porreca F, Vanderah TW. Constitutive activity at the cannabinoid CB1 receptor is required for behavioral response to noxious chemical stimulation of TRPV1: antinociceptive actions of CB1 inverse agonists. J Neurosci. 2008; 28:11593–11602. [PubMed: 18987195]

67. Chin CN, Lucas-Lenard J, Abadji V, Kendall DA. Ligand binding and modulation of cyclic AMP levels depend on the chemical nature of residue 192 of the human cannabinoid receptor 1. J Neurochem. 1998; 70:366–373. [PubMed: 9422383]

68. Song ZH, Bonner TI. A lysine residue of the cannabinoid receptor is critical for receptor recognition by several agonists but not WIN55212-2. Mol Pharmacol. 1996; 49:891–896. [PubMed: 8622639]

69. Kjelsberg MA, Cotecchia S, Ostrowski J, Caron MG, Lefkowitz RJ. Constitutive activation of the alpha 1B-adrenergic receptor by all amino acid substitutions at a single site. Evidence for a region which constrains receptor activation. J Biol Chem. 1992; 267:1430–1433. [PubMed: 1346134]

70. Huang P, Li J, Chen C, Visiers I, Weinstein H, Liu-Chen LY. Functional role of a conserved motif in TM6 of the rat mu opioid receptor: constitutively active and inactive receptors result from substitutions of Thr6.34(279) with Lys and Asp. Biochemistry. 2001; 40:13501–13509. [PubMed: 11695897]

71. Tao YX, Abell AN, Liu X, Nakamura K, Segaloff DL. Constitutive activation of G protein-coupled receptors as a result of selective substitution of a conserved leucine residue in transmembrane helix III. Mol Endocrinol. 2000; 14:1272–1282. [PubMed: 10935550]

72. Nikiforovich GV, Baranski TJ. Structural mechanisms of constitutive activation in the C5a receptors with mutations in the extracellular loops: molecular modeling study. Proteins. 2012; 80:71–80. [PubMed: 21960464]

73. Peeters MC, Li Q, van Westen GJ, Ijzerman AP. Three “hotspots” important for adenosine A(2B) receptor activation: a mutational analysis of transmembrane domains 4 and 5 and the second extracellular loop. Purinergic Signal. 2012; 8:23–38. [PubMed: 21818573]

74. Rasmussen SG, Choi HJ, Fung JJ, Pardon E, Casarosa P, Chae PS, Devree BT, Rosenbaum DM, Thian FS, Kobilka TS, Schnapp A, Konetzki I, Sunahara RK, Gellman SH, Pautsch A, Steyaert J, Weis WI, Kobilka BK. Structure of a nanobody-stabilized active state of the beta(2) adrenoceptor. Nature. 2011; 469:175–180. [PubMed: 21228869]

75. Rasmussen SG, DeVree BT, Zou Y, Kruse AC, Chung KY, Kobilka TS, Thian FS, Chae PS, Pardon E, Calinski D, Mathiesen JM, Shah ST, Lyons JA, Caffrey M, Gellman SH, Steyaert J, Skiniotis G, Weis WI, Sunahara RK, Kobilka BK. Crystal structure of the beta2 adrenergic receptor-Gs protein complex. Nature. 2011; 477:549–555. [PubMed: 21772288]

76. Standfuss J, Edwards PC, D'Antona A, Fransen M, Xie G, Oprian DD, Schertler GFX. The structural basis of agonist-induced activation in constitutively active rhodopsin. Nature. 2011; 471:660.

77. Xu F, Wu H, Katritch V, Han GW, Jacobson KA, Gao ZG, Cherezov V, Stevens RC. Structure of an agonist-bound human A2A adeno-sine receptor. Science. 2011; 332:322–327. [PubMed: 21393508]

78. Choe HW, Kim YJ, Park JH, Morizumi T, Pai EF, Krauss N, Hof-mann KP, Scheerer P, Ernst OP. Crystal structure of metarhodopsin II. Nature. 2011; 471:651–655. [PubMed: 21389988]

79. Yao X, Parnot C, Deupi X, Ratnala VR, Swaminath G, Farrens D, Kobilka B. Coupling ligand structure to specific conformational switches in the beta2-adrenoceptor. Nat Chem Biol. 2006; 2:417–422. [PubMed: 16799554]

80. Dror RO, Arlow DH, Borhani DW, Jensen MO, Piana S, Shaw DE. Identification of two distinct inactive conformations of the beta2-adrenergic receptor reconciles structural and biochemical observations. Proc Natl Acad Sci USA. 2009; 106:4689–4694. [PubMed: 19258456]

81. Pardo L, Deupi X, Dolker N, Lopez-Rodriguez ML, Campillo M. The role of internal water molecules in the structure and function of the rhodopsin family of G protein-coupled receptors. Chembiochem. 2007; 8:19–24. [PubMed: 17173267]

82. Angel TE, Chance MR, Palczewski K. Conserved waters mediate structural and functional activation of family A (rhodopsin-like) G protein-coupled receptors. Proc Natl Acad Sci USA. 2009; 106:8555–8560. [PubMed: 19433801]

83. Govaerts C, Bondue A, Springael JY, Olivella M, Deupi X, Le Poul E, Wodak SJ, Parmentier M, Pardo L, Blanpain C. Activation of CCR5 by chemokines involves an aromatic cluster between trans-membrane helices 2 and 3. J Biol Chem. 2003; 278:1892–1903. [PubMed: 12411445]

84. Javitch JA, Ballesteros JA, Weinstein H, Chen J. A cluster of aromatic residues in the sixth membrane-spanning segment of the dopamine D2 receptor is accessible in the binding-site crevice. Biochemistry. 1998; 37:998–1006. [PubMed: 9454590]

85. Jaakola VP, Griffith MT, Hanson MA, Cherezov V, Chien EY, Lane JR, Ijzerman AP, Stevens RC. The 2.6 angstrom crystal structure of a human A2A adenosine receptor bound to an antagonist. Science. 2008; 322:1211–1217. [PubMed: 18832607]

86. Park JH, Scheerer P, Hofmann KP, Choe HW, Ernst OP. Crystal structure of the ligand-free G-protein-coupled receptor opsin. Nature. 2008; 454:183–187. [PubMed: 18563085]

87. Scheerer P, Park JH, Hildebrand PW, Kim YJ, Krauss N, Choe HW, Hofmann KP, Ernst OP. Crystal structure of opsin in its G-protein-interacting conformation. Nature. 2008; 455:497–502. [PubMed: 18818650]

88. Dror RO, Arlow DH, Maragakis P, Mildorf TJ, Pan AC, Xu H, Borhani DW, Shaw DE. Activation mechanism of the beta2-adrenergic receptor. Proc Natl Acad Sci USA. 2011; 108:18684–18689. [PubMed: 22031696]

89. Porter JE, Hwa J, Perez DM. Activation of the alpha1b-adrenergic receptor is initiated by disruption of an interhelical salt bridge constraint. J Biol Chem. 1996; 271:28318–28323. [PubMed: 8910453]

90. Roth CB, Hanson MA, Stevens RC. Stabilization of the human beta2-adrenergic receptor TM4-TM3-TM5 helix interface by muta-genesis of Glu122(3.41), a critical residue in GPCR structure. J Mol Biol. 2008; 376:1305–1319. [PubMed: 18222471]

91. Sarkar CA, Dodevski I, Kenig M, Dudli S, Mohr A, Hermans E, Pluckthun A. Directed evolution of a G protein-coupled receptor for expression, stability, and binding selectivity. Proc Natl Acad Sci USA. 2008; 105:14808–14813. [PubMed: 18812512]

92. Leff P. The two-state model of receptor activation. Trends Pharmacol Sci. 1995; 16:89–97. [PubMed: 7540781]

93. Weiss JM, Morgan PH, Lutz MW, Kenakin TP. The cubic ternary complex receptor-occupancy model. III. resurrecting efficacy. J Theor Biol. 1996; 181:381–397. [PubMed: 8949584]

A

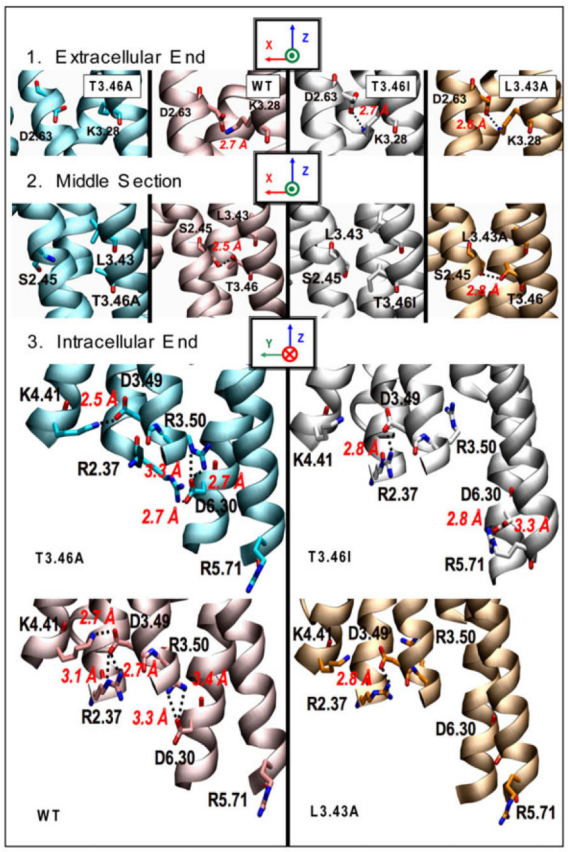

B

Receptor	Level of activity	R2.37 + D6.30 ionic lock	R3.50 + D6.30 ionic lock	D3.49 + K4.41 ionic lock	R5.71 + D6.30 ionic lock	D2.63 + K3.28 ionic lock
L3.43A	Highly active	No	No	No	No	Yes
T3.46I	Highly active	No	No	No	Yes	Yes
Wild-Type	Partially active	No	Yes	Yes	No	Yes
T3.46A	Fully inactive	Yes	Yes	Yes	No	No

Figure 1.

Predicted structures of the L3.43A, T3.46I, wild-type, and T3.46A receptors and their salt-bridge patterns. The consensus structure for the T3.46A (a), wild-type (b), T3.46I (c), and L3.43A (d) receptors are illustrated based on the low energy conformations from GEnSeMBLE MC computational predictions. Key salt bridge (R2.37 + D6.30, R3.50 + D6.30, D3.49 + K4.41, R5.71 + D6.30 and D2.63 + K3.28) and hydrogen bond (S2.45-T3.46) interactions in the consensus pattern are indicated by black dotted lines with red heteroatom distances. Note that the T3.46A receptor has a broken salt-bridge between D2.63 and K3.28 since the inter-residue distance is 6.8 Å. (**B**) Comparison of the key non-covalent interaction patterns for each receptor. Shaded cells indicate that this salt bridge interaction is also observed in the wild-type receptor.

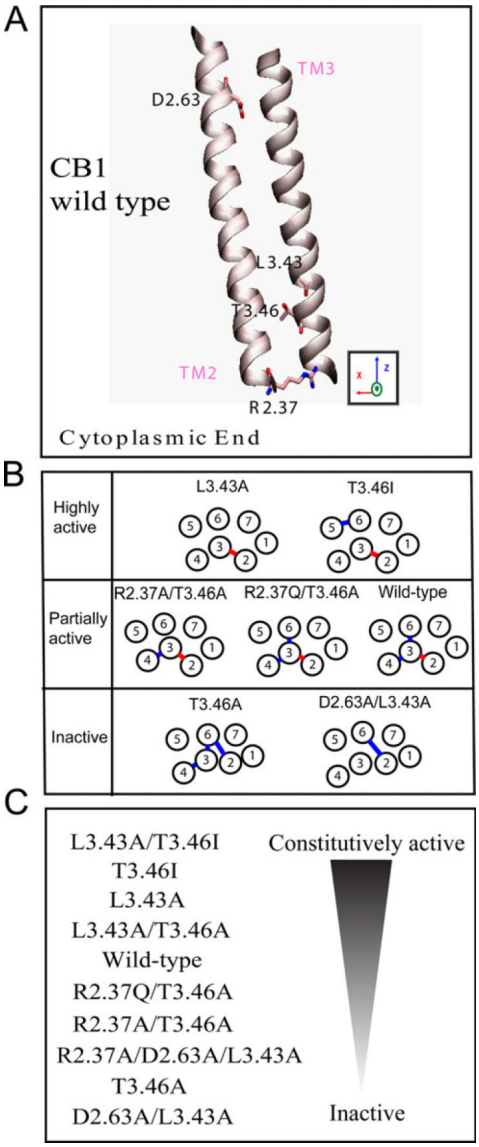

Figure 2.

Amino acids in TM2 and TM3 that are substituted to produce the single and double mutant receptors used in this study and comparison of the salt-bridge patterns of key CB1 receptors. (**A**) GEnSeMBLE MC predicted structures of TM2 and TM3 of the wild-type receptor are shown. The residues mutated in this study are labeled with the amino acid numbers denoting the Ballesteros-Weinstein nomenclature of the human CB1 receptor. (**B**) Comparisons of the key salt-bridges patterns of CB1 wild-type and mutant receptors. Blue lines connecting the TM helices indicate the pattern of intracellular salt-bridges identified by computational analysis (R2.37 + D6.30, R3.50 + D6.30, D3.49 + K4.41, and R5.71 + D6.30) as critical for various steps of receptor activation. The red line indicates a more extracellular salt-bridge (D2.63 + K3.28) critical for activation. Numbers in circles indicate the TM numbers for each receptor. The wild-type and mutant receptors are grouped by their predicted levels of constitutive activity; the highly active L3.43A and T3.46I receptors (top row); the partially active R2.37A/T3.46A, R2.37Q/T3.46A, and wild-type receptors (middle row); the inactive

T3.46A and D2.63A/L3.43A receptors (bottom row). (**C**) The single, double, and triple point mutant receptors proposed based on GEnSeMBLE MC computational predictions and evaluated for their biochemical properties are listed with a predicted rank order in terms of constitutive activity relative to the wild-type receptor.

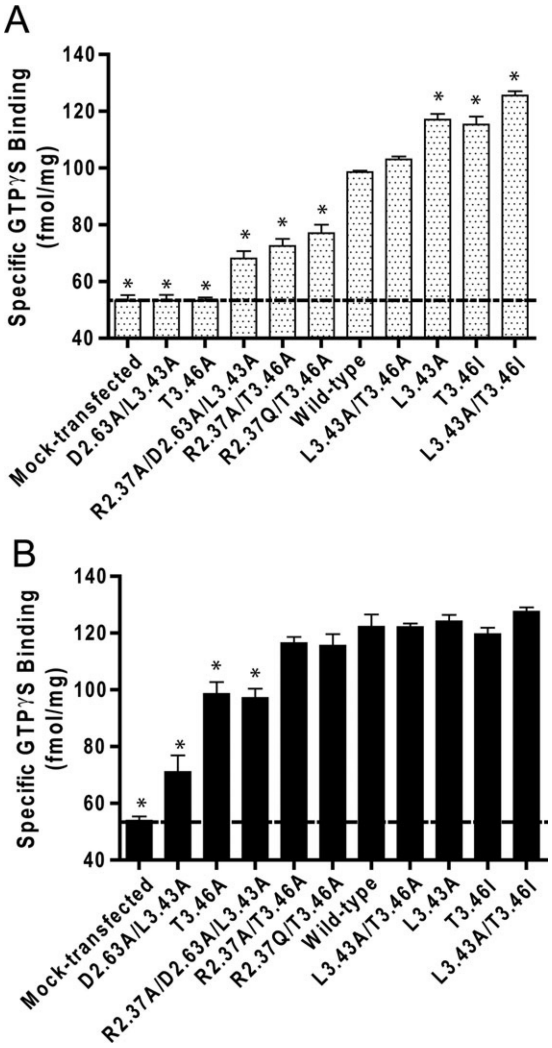

Figure 3.

Comparison of basal and agonist-induced GTPgS binding to HEK293 cell membranes expressing the CB1 wild-type and mutant receptors. (A) The level of [^{35}S]GTPgS binding was measured in the absence of ligand for the CB1 receptors to determine the level of basal activity. Data are presented as specific binding of GTPgS to the membrane. Nonspecific binding was determined in the presence of 10 m*M* unlabeled GTPgS. Each data point represents the mean ± S.E. (error bars) of at least three independent experiments performed in duplicate. (**B**) Comparison of agonist-induced GTPgS binding to HEK293 cell membranes expressing the CB1 wild-type and mutant receptors. The level of [^{35}S]GTPgS binding was measured in the presence (black bars) of 1 μ*M* CP55940 for the CB1 wild-type and mutant receptors. Nonspecific binding was determined in the presence of 10 m*M* unlabeled GTPgS. Each data point represents the mean ± SE (error bars) of at least three independent experiments performed in duplicate. The dashed line indicates the level of non CB1-mediated GTPgS binding obtained from [^{35}S]GTPgS binding to the mock-transfected membrane sample. The values for GTPγS binding from the mutant receptors are compared to the wild-type values using analysis of variance (ANOVA) followed by Bonferroni's post

hoc test for significance. *P* values of <0.05 were considered to be statistically significant and indicated by the asterisk (*).

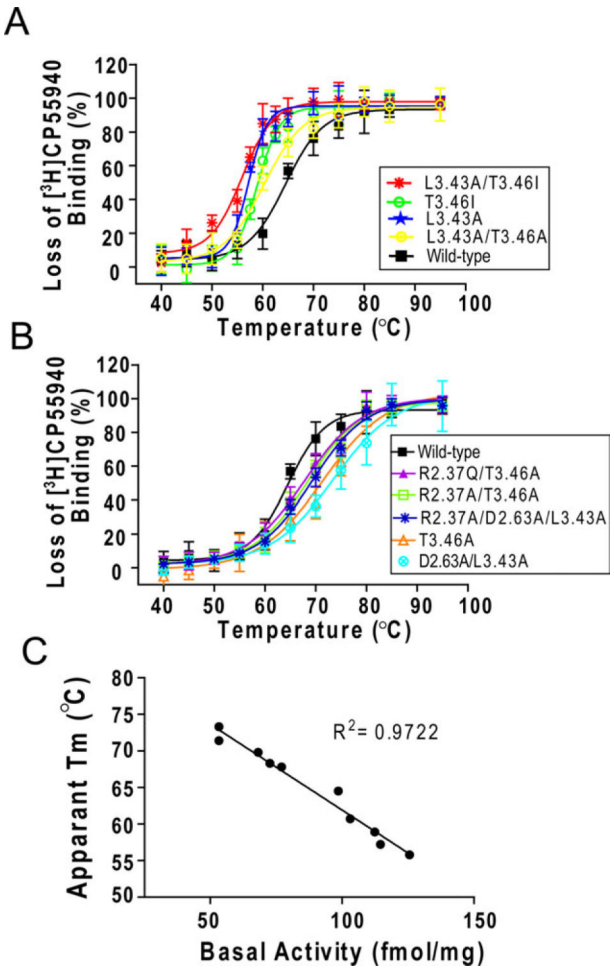

Figure 4.

Thermal stability of the CB1 wild-type and mutant receptors. The membrane prepared from HEK293 cells expressing the wild-type or mutant receptors was incubated at the indicated temperature for 30 minutes followed by cooling on ice as described in Materials and Methods. The residual binding capacity after heating the receptor relative to control was measured using [^{3}H]CP55940. The data are presented as the loss of [^{3}H]CP55940 binding relative to the control sample for each receptor (as described in Materials and Methods). (**A**) Receptors displaying lower apparent T_ms relative to the wild-type are shown. These include the L3.43A/T3.46I, T3.46I, L3.43A, and L3.43A/T3.46A receptors. (**B**) Receptors displaying higher apparent T_ms relative to the wild-type are shown with that of the wild-type receptor. These include D2.63A/L3.43A, T3.46A, R2.37A/D2.63A/L3.43A, R2.37A/T3.46A, and R2.37Q/T3.46A. Each data point in (A) and (B) represents the mean SE (error bars) of three independent experiments performed in duplicate. (**C**) Relation of T_m and the basal level of [^{35}S]GTPgS binding for all characterized receptors is shown. The line describes the trend. An R^2 value of 0.9722 indicates a good correlation between the thermal stability and G protein activation ability.

Table I

Apparent T*ms of the CB1 Wild-Type and Mutant Receptors*

Receptor	Apparent T_m (°C)
L3.43A/T3.46I	55.8 ± 1.2
T3.46I	58.1 ± 0.7
L3.43A	57.2 ± 1.6
L3.43A/T3.46A	60.7 ± 1.1
Wild-type	64.3 ± 0.8
R2.37Q/T3.46A	67.2 ± 0.9
R2.37A/T3.46A	68.1 ± 0.9
R2.37A/D2.63A/L3.43A	69.8 ± 1.2
T3.46A	71.7 ± 1.5
D2.63A/L3.43A	72.1 ± 2.1

The apparent T_m (mean ± SE) from thermal denaturation curves for each receptor was obtained from three individual experiments done in duplicate.

Table II

Ligand Binding Properties of the CB1 Wild-Type and Mutant Receptors

	[^{3}H]CP55940			[^{3}H]SR141716A		
	K_d (n*M*)	K_d ratio (receptor: wild-type)	B_{max} (fmol/mg)	K_d (n*M*)	K_d ratio (receptor: wild-type)	B_{max} (fmol/mg)
L3.43A/T3.46I	0.28 ± 0.02[a]	1:6	2603 ± 186	13.17 ± 1.72[a]	6:1	3637 ± 229
T3.46I	0.31 ± 0.04[a]	1:6	3933 ± 291	14.72 ± 2.10[a]	7:1	3621 ± 690
L3.43A	0.32 ± 0.13[a]	1:6	2974 ± 341	14.20 ± 1.87[a]	7:1	3859 ± 161
L3.43A/T3.46A	1.10 ± 0.23	1:1	2890 ± 108	7.50 ± 0.46[a]	4:1	3595 ± 205
Wild-type	1.78 ± 0.32		3724 ± 152	2.11 ± 0.42		4221 ± 284
R2.37A/T3.46A	5.58 ± 0.32[a]	3:1	3113 ± 263	1.67 ± 0.26	1:1	4310 ± 298
R2.37Q/T3.46A	6.21 ± 1.11[a]	3:1	3858 ± 444	1.59 ± 0.22	1:1	4627 ± 241
R2.37A/D2.63A/L3.43A	7.63 ± 0.89[a]	4:1	3201 ± 329	1.48 ± 0.20	1:1	4408 ± 303
T3.46A	9.83 ± 1.12[a]	6:1	3103 ± 280	0.61 ± 0.09[a]	1:3	4887 ± 210
D2.63A/L3.43A	12.74 ± 2.13[a]	7:1	3083 ± 405	0.64 ± 0.07[a]	1:3	3922 ± 159

Data are the mean ± SEM of three independent experiments performed in duplicate ($n = 3$ determinations).

[a]Statistically significant K_d differences from wild-type ($P < 0.05$) using analysis of variance (ANOVA) followed by Bonferroni's post hoc test.